JOURNAL OF OPTOELECTRONICS AND ADVANCED MATERIALS Vol. 10, No. 11, November 2008, p. 2876 - 2881

Combining thermo-photo elasticity for analysis of cracked bodies

L. MARSAVINA , E. M. CRACIUN[a*], R. A. TOMLINSON[b]
Politehnica University, Timisoara, 300222, Romania
[a]*Ovidius University, Constanța, 900527, Romania*
[b]*The University of Sheffield, Sheffield, S1 3JD, UK*

In recent years the possibility of using experimental stress analysis techniques like thermoelastic and photoelastic for determining the fracture mechanics parameters in cracked bodies has been highlighted. This has the advantage that photoelastic and thermoelastic measurements can be performed simultaneously. It is proposed that if both thermo- and photo- elastic data were taken simultaneously from the same crack and the stress intensity factor determined by the two different techniques then confidence could be obtained in the results. Such a procedure would have use where no analytical solution was available for verification purposes. An experiment was carried out to assess the potential and accuracy of using photo and thermo elastic stress analysis to determine the stress intensity factors. A central notch was machined into a steel cruciform specimen and a polymer coating was bonded adjacent to one end of the notch. The specimen was loaded in a biaxial test machine, thermoelastic and photoelastic data were recorded from the coating and stress intensity factors determined. This paper presents some results of the mixed mode stress intensity factors obtained by photoelasticity and thermo-elasticity for a sharp notch in the biaxial specimen.

(Received September 1, 2008; accepted October 30, 2008)

Keywords: Photoelasticity, Thermoelasticity, Stress intensity factor

1. Introduction

The stress intensity factors (SIFs) characterize the stress singularity around cracks and flaws. In fracture mechanics, these parameters are used to predict if the crack will become unstable by comparison with the fracture toughness.

Many experimental methods have been developed to determine the stress intensity factors. Photoelasticity is used for more than forty years, and is based on interpretation of the characteristic distributions of isochromatic fringe patterns around crack tips. Irwin [1] was the first to relate the maximum shear stress around crack tip to the value of the isochromatic at certain points. Smith [2] collected the photoelastic data on certain direction and used a linear interpolation between an apparent stress intensity factor and distance to the crack tip. The stress intensity factor is determined by extrapolation at the crack tip.

Nurse et al [3] used an algorithm based on the multiple – point – over deterministic method (MPODM). This algorithm is based on the Mukchelishvili's approach [4] to describe the stress field around the crack tip, using Fourier series. The theoretical solution describing the stress field is combined with the photoelastic results, given by the stress optic law, in order to obtain a series of simultaneous equations in which the unknowns are the parameters of the Fourier series. The system of equations is solved using a Newton – Raphson iteration scheme. This procedure was used to determine the mixed mode stress intensity factors for bi-material interface crack [5].

In the last two decades thermo-elasticity method has been developed to be a useful method in study of crack tip stress field. The use of thermoelastic data to study crack tip parameters was first proposed by Stanley and Chan [6] in 1986. They used the Westergaard equations to demonstrate a relationship between the stress intensity factors, K_I and K_{II} and the SPATE signal, S at a point (r, θ) from a crack tip. This relationship was developed into a graphical method to determine the crack tip parameters of a mode I fatigue crack. This technique was further developed on mode II fatigue cracks with limited success [7]. A study of simulated inclined edge and centre cracks by Stanley and Dulieu-Smith [8] showed that the lines of constant thermoelastic signal in the crack tip region generally took the form of a cardioid curve centred on the crack tip and, by determining the area and orientation of a typical cardioid, ΔK_I and ΔK_{II} were calculated. The method involved hand - fitting a cardiod shape to experimental data and subsequently the agreement between experiment and theory was concluded to be no better than moderate. An alternative approach for determining stress intensity factors for cracks subject to mixed-mode loading was developed by Tomlinson et al. [9, 10, 11]. A Newton-Raphson iteration combined with a least squares approach was used to fit the equations describing the stress field around the crack tip, based on Mushkelishvili' s approach, to the thermoelastic data.

Barone et al [12], highlights the possibility of using polymer coating as a strain witness for thermoelasticity. This has the advantage that photoelastic and thermoelastic measurements can be performed simultaneously, and the individual principal stresses can be evaluated. Industrial

applications of combining photo and thermo-elasticity are presented in [13]. Tomlinson et al. [14] shows that reliable values of stress intensity factors were obtained by thermoelasticity from photoelastic coating. However, to the author's knowledge there are less applications of combining photoelastic and thermoelastic techniques in order to determine the stress intensity factors [15, 16].

This study presents the results of stress intensity factors obtained by photoelasticity and thermoelasticity for a sharp notch in a biaxial specimen.

2. Stress intensity factors determination

The stress intensity factors for mixed mode cracks from the photoelastic measurements were calculated using the Nurse et al [3] algorithm based on the multiple – point – over deterministic method (MPODM) of Sanford et al [17]. Tomlinson et al. [9] developed a similar algorithm for determination of stress intensity factors from thermoelastic data. For both cases the algorithm is based on the Mukchelishvili's approach [4] to describe the stress field around the crack tip, using Fourier series. The theoretical solution describing the stress field is combined with the photoelastic or thermoelastic results, in order to obtain a series of simultaneous equations in which the unknowns are the parameters of the Fourier series. The system of equations is solved using a Newton – Raphson iteration scheme. Finally, the stress intensity factors are calculated using the parameters of the Fourier series. Practically, an array of approximately 75 data points are collected on radial lines from the map of isochromatic fringe order, thermoelastic map respectively, centered on the crack tip, and used to fit with the theoretical solution of the stress field [3,9,10]. The data should be in the singularity - dominated zone delimited by an inner and an outer limit.

3. Experimental procedure

3.1 Specimen and Biaxial test

The tests were performed on 150M36 steel cruciform specimen with a central spark-eroded slot inclined at 45^0 of length 2a = 36 mm, as in Fig. 1. The photoelastic coating PS-1D (supplied by Measurement Group Inc., USA) of 0.5 mm thickness was cut to cover half the surface of the specimen around one end of the notch and bonded using PC-1 adhesive. For the calibration of the thermoelastic data on the other side of the specimen was bonded a strain gauge rosette.

The load was applied using a 100 kN Denison Mayes Biaxial Testing Machine. This rig has four actuators, two providing vertical load and two providing horizontal load. The advantage of this test is that the mixed mode stress field can be easily produced by choosing the loads on the two axes, on a cruciform specimen with a 45^0 inclined crack or notch.

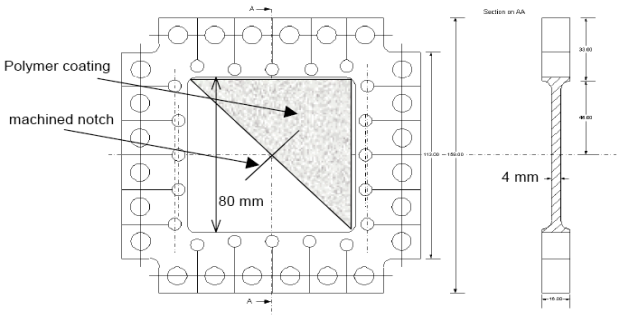

Fig. 1. The cruciform specimen with photoelastic coating around notch tip.

3.2 Photoelastic measurements

For the photoelastic measurements the load was applied statically, Table 1. In the first instance an equibiaxial load, which produce a Mode I stress field around the notch, was applied and the load was increased till a complete fringe loop appear. Four loads combinations on the two axes of the biaxial rig were used to produce different mixed mode ratios K_{II}/K_I equal to0.0, 1, 0.5, and 2. The photoelastic measurements were performed with a Reflection Polariscope 030 Series, manufactured by Measurements Group Inc. (USA), Fig. 2. Both light and dark field were used to observe the isochromatic fringe patterns at the crack tip. Typical photoelastic maps are shown in Fig. 3 corresponding to mode I load.

Fig. 2. Photoelastic measurements arrangement.

Table 1. Applied load for photoelastic measurements.

Static load				
File	P_x *kN*	σ_x *MPa*	P_y *KN*	σ_y *MPa*
M_0_1	16	85.33	16	85.33
M_05_2	12	32.00	36	96.00
M_1_3	0	0	40	106.67
M_2_4	-12	32.00	36	96.00

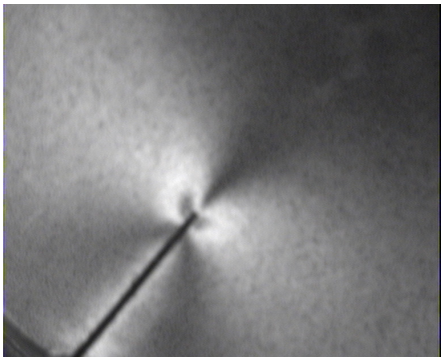

a) dark field

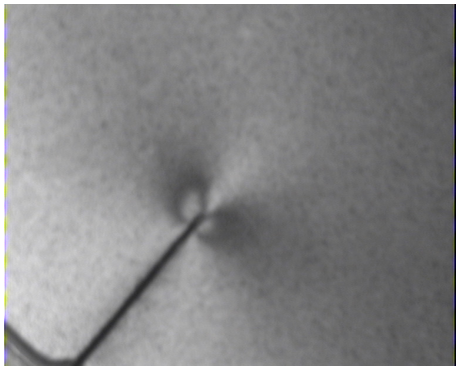

b) light field

Fig. 3. Photoelastic data maps for equi-biaxial loading ($P_x = P_y = 16$ kN, $K_{II}/K_I=0$).

The phase-stepping method of Patterson et al [18] was performed in order to determine the fractional fringe order and isoclinic parameter. The polarized light is directed to the specimen passing the polariser and the inner quarter wave plate. The beam passed trough the coating and is reflected back passing the outer quarter wave plate and the analyzer. The image from the analyzer is focused a CCD camera by a standard camera lens. Six phase - stepped images were recorded by changing the orientation of the analyzer and output quarter wave plate. The six sets of images, each 256 x 256 are calibrated and unwrapped using the algorithm of Wang et al [19]. In order to calculate the stress intensity factors the crack tip position needs to be determined. The program generates an array of data which contain the coordinate of points and the fringe order.

3.3 Thermoelastic measurements

The thermoelastic measurements were performed using a DeltaTherm 1000 system, manufactured by Stress Photonics Inc. (USA). The applied cyclic load, sine waveforms, was lower than the load used for photoelasticity in order to prevent crack growing from the notch. The configuration of the experimental arrangement is shown in Fig. 4. The infrared camera acquires thermal images from the coated specimen surface. The Lock In – Amplifier correlate the signal from detector with a reference signal took from one of the loading cells of the biaxial machine. A computer and DeltaVision software control the aquisition process.

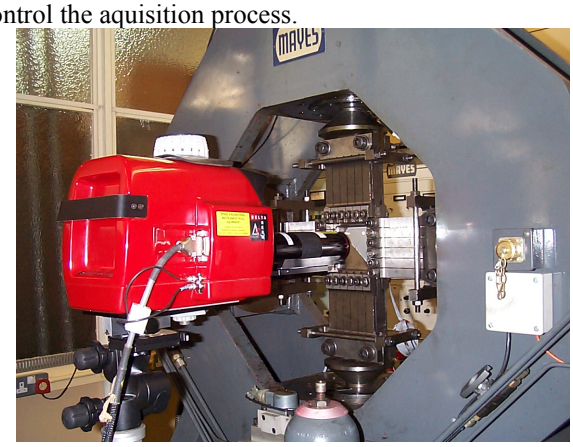

Fig. 4. Thermoelastic experiment arrangement.

Four different combinations of the applied loads on the X and Y axes of the test machine where used in order to produce different mixity of K_{II}/K_I, Table 2.

The frequency of the tests was 8 Hz, which produce a well-defined cycle and in the same time assure the adiabatic conditions for the thermoelastic measurements. The shape of the load waveforms and the response from the loading cells were checked using two oscilloscopes.

Table 2. Applied load for thermoelastic measurements.

Cyclic load with sinusoidal waveform								
Scan	P_{xmin} *kN*	P_{xmax} *kN*	R_x -	$\Delta\sigma_x$ *MPa*	P_{ymin} *KN*	P_{ymax} *kN*	R_y -	$\Delta\sigma_y$ *MPa*
718_1	0.1	6.009	0.017	15.758	0.13	5.968	0.022	15.568
718_1_4	0	0	0	0	0.18	14	0.013	36.854
718_05_5	0	3	0	8	0.06	8.95	0.007	23.7
718_2_6	2.943	0.1	0.033	-7.581	0.08	8.923	0.009	23.582

Thermoelastic data was collected from the coating using a zoom lens in wide-angle position, and the parameters of data acquisition were: Integration time: 3.25 min, Electronic shutter: 98 %. The thermoelastic signal was calibrated using two orthogonal strain gauge rosette bonded on the opposite side of the specimen to the coating, in a region of constant stress. All the test parameters (frequency, integration time, electronic shutter,

zoom lens) were the same for the calibration test and for the thermoelastic measurements around notches. Typically thermoelastic map are shown in Fig. 5 for pure mode I loading ($\Delta K_{II}/\Delta K_I$=0.0) and mixed mode ($\Delta K_{II}/\Delta K_I$=1.0).

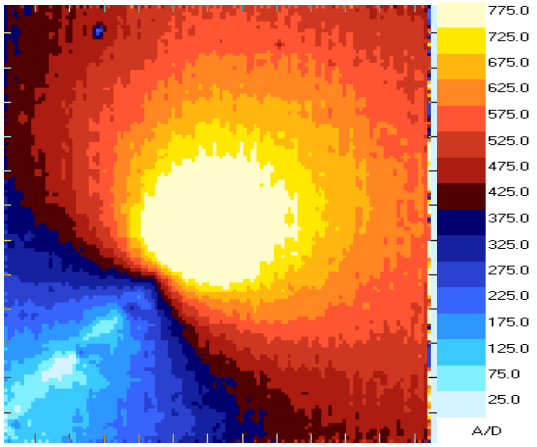

a) $\Delta K_{II}/\Delta K_I$=0.0

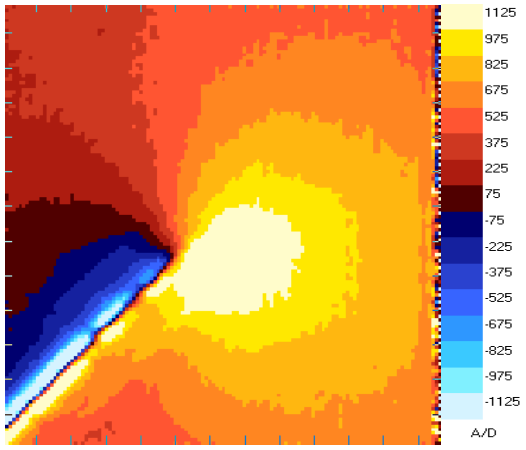

b) $\Delta K_{II}/\Delta K_I$=1.0

Fig. 5. Thermoelastic data maps.

4. Stress intensity factors results and conclusions

The stress intensity factors from reflection photoelasticity were determined according with Nurse – Patterson algorithm and using phase stepping photoelasticity [18, 19] and WinVision code. The experimental results are compared with the analytical solution [20]. The stress intensity factors results from photoelaticity are affected by a relative error between 0.9 % to 5.5 %.

Each thermoelastic map was interrogated at approximately 80 points. The coordinates of these points and the thermoelastic signal were used to calculate the stress intensity factors ΔK_I and ΔK_{II} using the Tomlinson et al [9] method. This method requires thermoelastic data to be taken from the "singularity-dominated zone", where the principles of linear elastic fracture mechanics are valid. In this purpose the thermoelastic map obtained from each scan was interrogated at a number of points on radial lines radiating from the crack tip between an inner and an outer limit. The inner limit should mask the plastic, triaxial and non-adiabatic effects around the crack tip. The outer limit represents the extension of the singularity-dominated zone. For the case of using polymer coating for thermoelastic measurements the edge effect should be taken into account. It is considered that data are affected by the edge effect, on a region about 4 times thickness of the coating, by the mismatch of the Poisson's ratio. For this case using a 0.5 mm coating data were collecting only from 2 mm to the edge. The outer limit was considered using 0.4 from the notch length (0.4 x 18 mm = 7.2 mm).

The results were compared to those determined from theory [20] in Fig. 6. This shows the experimental stress intensity factors normalised with theoretical values for different applied mixed mode stress intensity factors. The values of the experimental and theoretical stress intensity factors are also given in Table 4. The quality of the fit of the stress field equations to the experimental data expressed by the two statistical parameters which are the mean and variance of the squared residuals are also presented in Table 4.

Table 3. Stress intensity factors results from photoelastic measurements.

File	Theoretical values			Experimental values			Statistical parameters	
	K_{Ithe} $MPa\sqrt{m}$	K_{IIthe} $MPa\sqrt{m}$	$\frac{K_{IIthe}}{K_{Ithe}}$	K_{Iexp} $MPa\sqrt{m}$	K_{IIexp} $MPa\sqrt{m}$	$\frac{K_{II\,exp}}{K_{I\,exp}}$	Mean	Variance
M_0_1	3.739	0.023	0.006	3.783	0.024	0.006	0.009	0.004
M_05_2	4.399	4.399	1.000	4.407	4.227	0.959	0.001	0.016
M_1_3	3.785	1.875	0.495	3.662	1.981	0.541	0.001	0.004
M_2_4	1.910	3.720	1.948	2.021	3.826	1.893	0.013	0.005

Table 4. Stress intensity factors results from thermoelastic measurements.

Scan	Theoretical values			Experimental values			Statistical parameters	
	ΔK_{Ithe} $MPa\sqrt{m}$	ΔK_{IIthe} $MPa\sqrt{m}$	$\frac{\Delta K_{IIthe}}{\Delta K_{Ithe}}$	ΔK_{Iexp} $MPa\sqrt{m}$	ΔK_{IIexp} $MPa\sqrt{m}$	$\frac{\Delta K_{II\,\exp}}{\Delta K_{I\,\exp}}$	Mean	Variance
718_1	3.739	0.023	0.006	3.783	0.024	0.006	0.009	0.004
718_1_4	4.399	4.399	1.000	4.407	4.227	0.959	0.001	0.016
718_05_5	3.785	1.875	0.495	3.662	1.981	0.541	0.001	0.004
718_2_6	1.910	3.720	1.948	2.021	3.826	1.893	0.013	0.005

In the thermoelastic maps presented in Fig. 5 the edge effect along the notch produced by the Poison's ratio mismatch can be observed. This effect was taken into account when the data for stress intensity factor determination were collected.

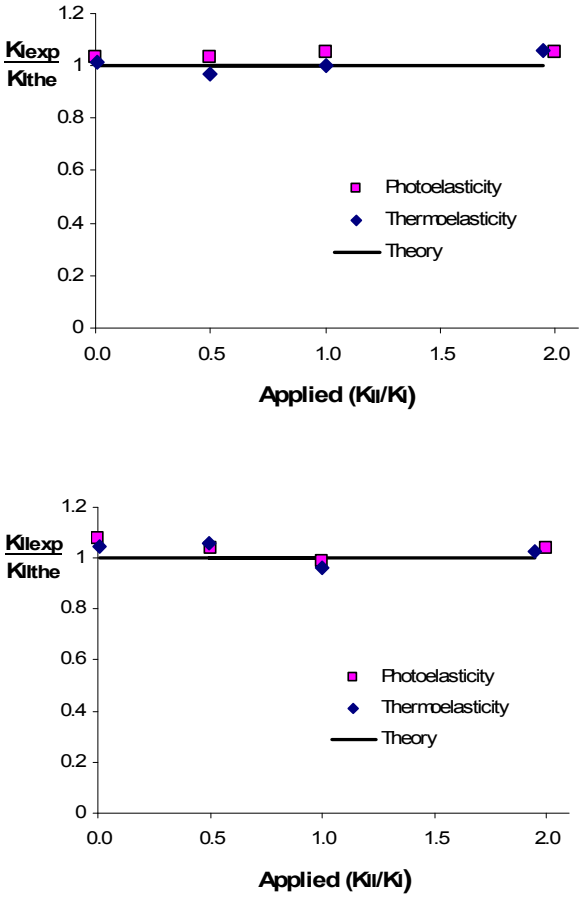

Fig. 6. Stress intensity factor results from photo and thermo elasticity measurements.

It was observed that the thermoelastic signal obtained from the coating is attenuated. Barone and Patterson [12] estimated that the signal from coating is around 5 times attenuated to the signal obtained from black matt-sprayed surfaces. Anyway, this doesn't affect the accuracy of the method if the calibration constant is correctly determined.

However, the obtained experimental results of the stress intensity factors are in good agreement with those theoretical values, Fig. 6. The maximum error for ΔK_I is 5.8% obtained for applied $\Delta K_{II}/\Delta K_I = 1.948$ and for ΔK_{II} is 5.6 % for $\Delta K_{II}/\Delta K_I = 0.495$. All other results are within 5% error between theoretical and experimental values of the stress intensity factors.

The experimental results have shown that the polycarbonate coatings can be used successful for thermoelastic measurements as a strain witness.

Both Photo and Thermo elasticity are full field and non contact experimental stress analysis methods. This paper shows that the thermoelastic data could be recorded from the birefringent coating, which allows combining the two experimental techniques. If photoelasticity gives the difference of the principal stresses thermoelasticity measures the sum of the principal stresses. By combining the two techniques stress separation became very simple by addition and extracting of photo and thermo data.

However thermoelasticity is a quasi-static stress measurement and requires a dynamic load to extract the thermoelastic signal in phase with the applied load, while photoelasticity is a static stress measurement. It is recommended that the photoelastic measurements to be performed at the mean load of the dynamic load for thermoelastic measurements.

A further advantage is in the validation of the too methods against each other.

Acknowledgements

This work was supported by EPSRC Grant No. GR-N32792-01 and Department of Mechanical Engineering, University of Sheffield, United Kingdom.

References

[1] G. R. Irwin Expt. Stress Anal., (S.E.S.A) **16**(1), 69-96 (1958).
[2] D. G. Smith, C. W. Smith, C. W. Engng. Fract. Mechs. **4**, 357 (1972).
[3] A. D. Nurse, E. A. Patterson, Fatigue Fract. Engng. Mater. Struct. **16**(12), 1339 (1993).
[4] N. I. Muskhelishvili, Some basic problems of the mathematical theory of elasticity, 3rd edn., Noordhoff, Groningen (1963).
[5] M. J. Ekman, L. Marsavina, A. D.Nurse, Fatigue Fract. Engng. Mater. Struct., **23**, 619 (2000).
[6] P. Stanley, W. K. Chan, Proc. SEM Spring Conf. on Expt. Mechanics, New Orleans, 916 – 923 (1986).
[7] P. Stanley, W. K. Chan, Proc. Int. Conf. on Fatigue of Engng. Mater. Struct., IMechE., 105 – 114 (1986).
[8] P. Stanley, J. M. Dulieu – Smith, Proc. SEM Spring Conf. on Expt. Mechanics, Dearborn, 617 – 626 (1993).
[9] R. A. Tomlinson, A. D. Nurse, E. A. Patterson, Fatigue Fract. Engng. Mater. Struct. **20**(2), 217 (1997).
[10] R. A. Tomlinson, L. Marsavina, Exp. Mech, **44**(5), 487 (2004).
[11] L. Marsavina, R. A. Tomlinson, J. Optoelectron. Adv. Mater. **6**(4), 1323 (2004).
[12] S. Barone, E. A. Patterson E. A., J. Strain Anal **33**(3), 223 (1998).
[13] R. J. Greene, E. A., Proc. 2002 SEM Conf. Expt. Applied Mechanics, Milwaukee, #101 (2002)
[14] R. A. Tomlinson, R. J. Greene, E. A. Patterson, L Marsavina, Proceedings of SEM 2003 Conference, #170 (2003).
[15] D. F. Woolard, M. K. Hinders, Proceedings of SPIE, **3587**, 88 (1999).
[16] A. Shimamoto, H. Ohkawara, H. Zhao, Key Engng. M., **324 – 325**, 1103 (2006).
[17] R. J. Sanford, J. W. Dally (1978). NLR Report 8202, Washington DC (1978).
[18] E. A. Patterson, Z. F. Wang, Strain **72**, 49 (1991).
[19] Z. F. Wang, E. A. Patterson, Opt. Laser Eng. **22**, 91 (1995).
[20] H. Gao, N. Alagok,, M. W. Brown, K. J. Miller, ASTM STP 853, Miller K. J. and Brown M. W. Eds. ASTM, Philadelphia, 184-202 (1985).

*Corresponding author: mcraciun@univ-ovidius.ro